JOM, Vol. 74, No. 5, 2022
https://doi.org/10.1007/s11837-022-05215-1

Efficient Extraction of Manganese from Low-Grade Pyrolusite by a Sawdust Pyrolysis Reduction Roasting-Acid Leaching Process

JINRONG JU,[1,2,3,4] YALI FENG,[1,5] HAORAN LI,[2,3] and XIAOFENG ZHONG[1]

1.—Civil and Resource Engineering School, University of Science and Technology Beijing, Beijing 100083, China. 2.—Key Laboratory of Biochemical Engineering, Institute of Process Engineering, Chinese Academy of Sciences, Beijing 100190, China. 3.—University of Chinese Academy of Sciences, Beijing 100049, China. 4.—e-mail: jjrong0906@163.com. 5.—e-mail: ylfeng126@126.com

In this work, a novel method for extraction of manganese from low-grade pyrolusite by a sawdust pyrolysis reduction roasting-acid leaching process was explored. The reduction roasting was studied systematically, and the mechanism was also explored by thermodynamic and phase change analysis. Results indicate that sawdust was rapidly pyrolyzed at 250–450°C to generate a large amount of reducing gases such as CO, CH_4, and H_2, which gradually reduced MnO_2 in low-grade pyrolusite to MnO. The reduction process of MnO_2 was identified as $MnO_2 \rightarrow Mn_2O_3 \rightarrow Mn_3O_4 \rightarrow MnO$. It was proved that MnO_2 of low-grade pyrolusite could be reduced effectively to MnO at lower temperature and shorter duration time by sawdust pyrolysis. Meanwhile, the optimum leaching efficiency of 99.45% for manganese could be attained when sawdust dosage was 11% of the mass of low-grade pyrolusite, the roasting temperature was 500°C, and the roasting time was 25 min.

INTRODUCTION

Renewable energy, as a feasible substitute for fossil fuels and a means to reduce the harmful effects of fossil fuel combustion emissions, has become more and more popular.[1] Among many renewable energy sources such as solar energy, wind energy, hydropower, biomass energy, and biofuels, biomass energy is the oldest known energy source in the world and the only carbon source produced by non-fossil fuels.[2,3] Biomass-based renewable energy is clean and safe, which is conducive to protecting the environment, energy security, and economy. The main environmental benefit provided by biomass energy utilization is recycling CO_2 emitted from biomass combustion by reintroducing it into the photosynthesis cycle, without causing net greenhouse gas emissions.[4] It is generally accepted that biomass is regarded as the only carbon-containing resource that can partially replace fossil fuels.[5,6] Biomass can be converted into tristate fuels and chemicals through thermochemical processes including pyrolysis, direct combustion, solidification, liquefaction, and gasification means, among which pyrolysis has received increasing attention, since the process conditions may be optimized to produce high energy density pyrolytic oils in addition to derived charcoal and gas.[7]

Among the reported technologies of biomass utilization, biomass pyrolysis technology has attracted extensive attention in the field of mineral reduction, mainly using renewable biomass to replace traditional coal reducing agents to further reduce valuable metals in minerals.[8] For example, Yue et al.[9] studied the thermal reduction desorption of cadmium in contaminated soil by biomass pyrolysis, and the results showed that when the mixture of biomass and contaminated soil was pyrolyzed at about 550°C, the gases in the biomass pyrolysis products (such as CO and hydrocarbon gases) could

(Received December 2, 2021; accepted February 8, 2022; published online February 28, 2022)

chemically reduce Cd(II) to volatile Cd^0; Huang et al.[10] explored the process of direct reduction of high-phosphorus oolitic hematite by biomass pyrolysis, and determined that when the mass ratio of iron ore to biomass was 1:0.6, the reduction temperature was 1100°C, and the reduction time was 55 min, the metallization ratio of hematite reached over 99%. The sulfur, nitrogen content, and ash content of biomass energy are lower than coal, and the hydrogen content of biomass energy is higher.[11,12] Compared with traditional coal reductant, biomass pyrolysis reduction can effectively reduce the emissions of acid gases (NO_x and SO_x) and greenhouse gases.[13,14] Moreover, in the traditional carbon reduction process, heat is transferred from the outside to the inside, which cannot effectively supplement the heat consumed by the reaction. Therefore, the temperature in the center of the particle is lower than the outside temperature, forming a "cold center" phenomenon, which reduces the metal reduction efficiency.[11] However, when biomass is used as the reducing agent, during the reduction process the reducing gas generated by pyrolysis of biomass reacts with minerals, and the reduction efficiency of this process is better.

Manganese (Mn) is the fourth most commonly used metal on the earth, and is widely used in iron and steel metallurgy, the chemical industry, electronics, batteries, and other manufacturing industries.[15–17] Manganese is usually produced by electrodeposition of manganese from sulfate solution.[18] Manganese ores in nature are mainly rhodochrosite and pyrolusite, and their main components are $MnCO_3$ and MnO_2, respectively.[19] However, 93.6% of manganese ore reserves in China are low-grade pyrolusite (Mn% < 30%). At present, with the development of industry, the demand for manganese alloy is increasing and import pressure is increasing.[12] Therefore, in order to alleviate the current import pressure and ensure the sustainable production of manganese products, the efficient leaching and utilization of low-grade pyrolusite has attracted extensive attention.

Pyrolusite is stable under acidic or alkaline conditions, but manganese can be extracted by acid under reducing conditions due to the formation of acid-soluble manganese oxides.[20] Generally, extracting manganese from pyrolusite includes pyrometallurgical reduction roasting and hydrometallurgical reduction leaching.[21,22] The hydrometallurgical reduction method has a series of problems such as low efficiency, low extraction efficiency, and large consumption of reducing agent, which obviously is not suitable for extracting manganese from low-grade pyrolusite. Based on the observation that biomass can be pyrolyzed into laevoglucose, uronic acid, acetic acid, wood vinegar, and other low-molecular-weight organic compounds at 250–300°C,[23,24] we previously presented an article about reductive leaching of manganese from low-grade pyrolusite ore in sulfuric acid solution using pyrolysis-pretreated sawdust as a reductant.[25] Although this process can replace traditional coal as a reducing agent to extract manganese from low-grade pyrolusite, there are some shortcomings such as the large amounts of sawdust and sulfuric acid required, and a high leaching temperature. The roasting reduction can be achieved using coal-based reductant,[26,27] pyrite,[28,29] other reducing substances, or gases such as sulfur[30] or carbon monoxide[31] at high temperature. These reduction methods have some disadvantages, such as high energy consumption, poor operating conditions, and serious environmental pollution.[32] In recent years, a large number of studies have shown that biomass such as corn stalks, walnut shells, cassava, sugar cane, banyan leaves and tea as reducing agents can reduce MnO_2 in pyrolusite.[11,33–38] The reason that biomass can be used as reductant of pyrolusite is that biomass will be rapidly pyrolyzed to produce carbon monoxide (CO), methane (CH_4), hydrogen (H_2), and biochar (C) with strong reducibility in the process of roasting in the absence of oxygen.[39–41]

Hence, considering the defects of a low utilization ratio of sawdust and the large consumption of sulfuric acid in previous work, and that sawdust, as a clean energy source, can be pyrolyzed to produce a large amount of reducing gas at a low temperature, this study investigated the extraction of manganese from low-grade pyrolusite by a sawdust pyrolysis reduction roasting-acid leaching process. That is, firstly, sawdust and low-grade pyrolusite are mixed and roasted together, and manganese dioxide (MnO_2) in the low-grade pyrolusite is reduced to manganous oxide (MnO), and then sulfuric acid leaching is carried out. The effects of sawdust dosage, roasting temperature, and roasting time on manganese leaching efficiency were systematically investigated by orthogonal experiments and single factor conditional experiments. At the same time, thermogravimetric analysis (TG), derivative thermogravimetry (DTG) and x-ray diffraction (XRD) were used to study the chemical reaction behavior and phase structure change of manganese during the reduction process. Moreover, based on the analysis of the pyrolysis characteristics of sawdust, the thermodynamic characteristics of reduction roasting, the quality index and the phase change of roasted products, and the mechanism for recovering manganese from low-grade pyrolusite by a sawdust pyrolysis reduction roasting-acid leaching process is put forward. This research not only realizes the utilization of waste sawdust, but also recovers manganese from low-grade pyrolusite, reducing energy consumption and bringing good economic benefits.

MATERIALS AND METHODS

Materials

In this study, low-grade pyrolusite was provided by a mining company in Hunan Province, China.

Table I. Chemical composition of low-grade pyrolusite

Element	Mn	Si	Fe	Al	Mg	Ca	P	S
Content/%	28.42	18.44	5.78	4.57	0.83	0.35	0.09	0.03

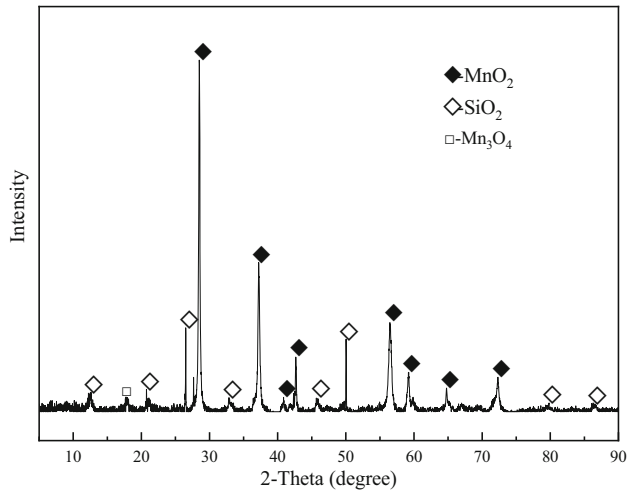

Fig. 1. XRD pattern of low-grade pyrolusite.

The low-grade pyrolusite samples were ground to below 0.074 mm and dried at 85°C for 90 min, and were characterized by x-ray fluorescence (XRF: Axios, PANalytical B.V., Almelo, the Netherlands) under the following conditions: non-attenuating 4-kW x-ray tube, 60-kW solid-state generator power, and 160-mA current; and x-ray diffraction (XRD: Smartlab, Rigaku Corporation, Tokyo, Japan) at a scan range of 5° to 90° 2θ at a rate of 5° min^{-1}. The results are shown in Table I and Fig. 1, respectively. According to Fig. 1, low-grade pyrolusite is mainly composed of manganese dioxide (MnO_2), quartz (SiO_2), and a small amount of manganous-manganic oxide (Mn_3O_4). As shown by XRF results in Table I, low-grade pyrolusite mainly contains 28.42% manganese (Mn), 18.44% silicon (Si), 5.78% iron (Fe) and 4.57% aluminum (Al) as well as a small amount of magnesium (Mg), calcium (Ca), phosphorus (P) and sulfur (S). The sawdust used in the experiment came from a furniture factory in Beijing, and its particle size was less than 5 mm. The chemical element contents of the sawdust was tested with an element analyzer (Vario MACRO cube). Chemical element analysis indicated that the sawdust was composed of 44.07% carbon (C), 36.87% oxygen (O), 5.26% hydrogen (H), 1.18% nitrogen (N) and 0.09% sulfur (S). The elemental analysis of the sawdust was provided by the Advanced Analysis and Measurement Center of the Institute of Process Engineering, Chinese Academy of Sciences (Beijing, China).

Experimental Procedures

Figure 2 shows a schematic diagram of the experimental device. It mainly includes roasting equipment and a leaching device. In this study, sawdust, a type of biomass, was used as the reducing agent to roast with low-grade pyrite in an oxygen-free environment. Manganese dioxide (MnO_2) in low-grade pyrolusite was reduced to manganous oxide (MnO) by reducing substances generated in the sawdust pyrolysis process, so manganese was extracted by sulfuric acid leaching. The detailed experimental procedure is as follows. Firstly, low-grade pyrolusite and sawdust were mixed evenly according to a certain mass ratio (the mass of sawdust accounts for 6–13% of that of low-grade pyrolusite) and put into a porcelain boat; the porcelain boat was put into a tube furnace. Then, N_2 was introduced into the tube furnace to remove the oxidizing atmosphere. In the whole experiment, the temperature in the tube furnace was raised to a predetermined temperature (350–500°C) at a heating rate of 30°C min^{-1}, and maintained at this temperature for a period of time (10–35 min). After roasting, the roasted product was taken out after it had cooled to room temperature. The roasting slag obtained under different roasting conditions was characterized by x-ray diffractometry at a scan range of 5° to 90° 2θ at a rate of 5° min^{-1}. Finally, a certain amount of roasting slag was leached for 120 min with 1.5 mol/l H_2SO_4 solution at 80°C and a liquid-solid mass ratio of 10:1. The leaching residue was dried and weighed, and then ground to below 0.074 mm. A 0.2-g sample, finely ground, was completely dissolved in mixed acid (20 ml sulfuric acid, 5 ml nitric acid, 0.5 ml hydrofluoric acid) and diluted to 100 ml. The concentration of manganese in solution was determined by inductively coupled plasma emission spectrometry (ICP-OES: iCAP 6300, Thermo Scientific). According to the concentration of manganese in the solution, the content of manganese in the leaching residue was determined. Similarly, manganese content in roasted slag was determined by this method. Based on the principle of conservation of mass, the leaching efficiency of manganese was calculated by the following Eq. 1:

$$E(\%) = \left(1 - \frac{m_1 w_1}{m_0 w_0}\right) \times 100\% \qquad (1)$$

where E is the leaching efficiency of manganese; m_0 and m_1 are the mass of roasting slag and leaching residue participating in the leaching reaction,

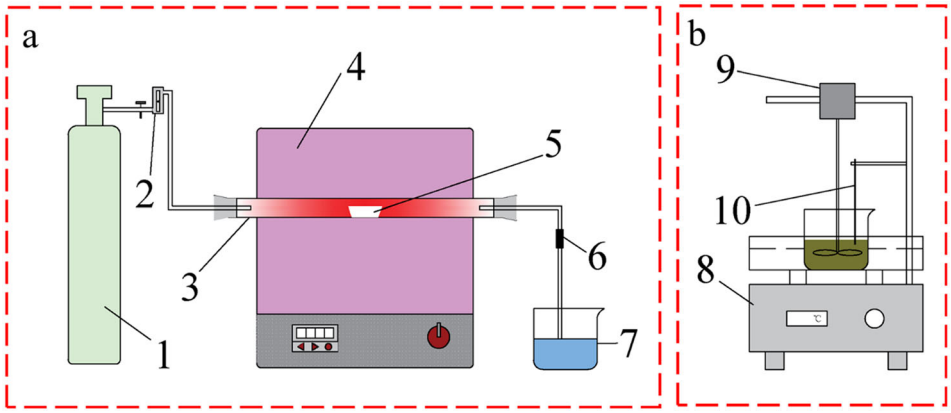

Fig. 2. Schematic diagram of experimental device: (a) roasting device, (b) leaching device. *1* Nitrogen cylinder, *2* rotameter, *3* quartz tube, *4* tube furnace, *5* porcelain boat, *6* condensing device, *7* tail gas collection device, *8* hotplate stirrer, *9* stirrer, *10* temperature sensor.

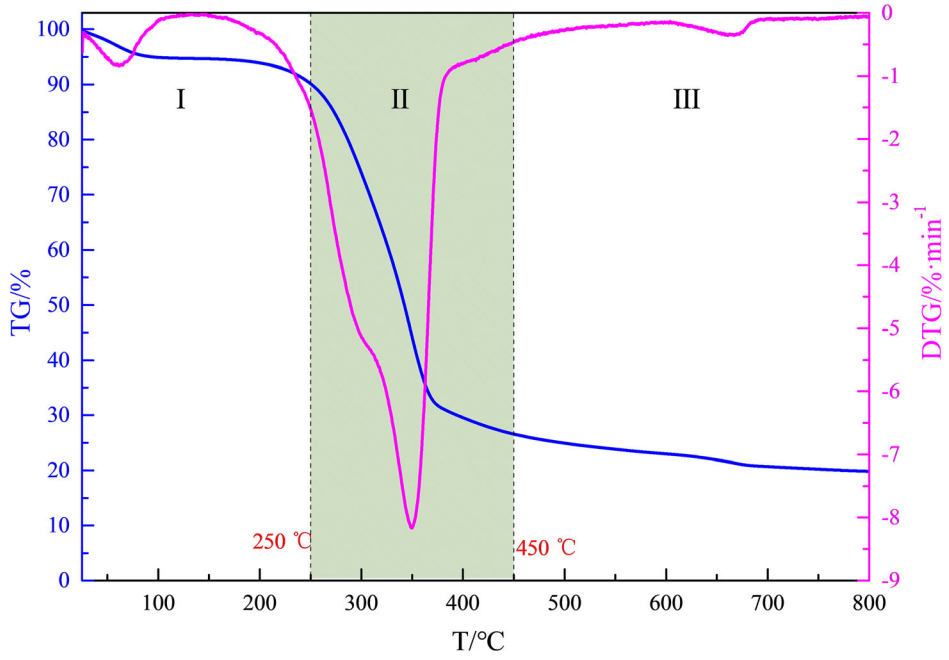

Fig. 3. TG and DTG curves of sawdust.

respectively; and w_0 and w_1 refer to the manganese concentration in roasting slag and leaching residue, respectively.

RESULTS AND DISCUSSION

Pyrolysis Characteristics of Sawdust

The thermogravimetric analysis of sawdust (METTLER TOLEDO, Switzerland) was performed under protective gas at a 100 ml/min flow rate. Figure 3 is the thermogravimetric analysis curve of sawdust. According to the thermogravimetric curve of sawdust pyrolysis, pyrolysis of sawdust can be divided into three stages: the first stage (0–250°C) is mainly the loss stage of free water and bound water in sawdust. The TG curve drops rapidly, and a peak is observed on the DTG curve at 0–100°C, which is due to the rapid evaporation of free water in sawdust in this temperature range. The bound water in sawdust is constantly lost at temperatures of 100–250°C, with the TG curve slowly decreasing.[12] The second stage (250–450°C) is the main stage of sawdust pyrolysis, during which the sawdust structure changes. The TG curve drops rapidly, and a very sharp trough is observed on the DTG curve. The structural components of sawdust, cellulose, hemicellulose, and lignin undergo corresponding pyrolysis reactions at their corresponding pyrolysis temperature ranges, producing a large number of small molecular gases.[11,42,43] The volatile gas components produced by pyrolysis of sawdust at 350°C are analyzed by a gas chromatograph-mass

spectrometer (GC-MS: Thermo Fisher Trace1300-ISQ) to calculate the relative contents of CO, CO_2, CH_4, and H_2. The analysis results show that it mainly includes 26.42% carbon monoxide (CO), 65.74% carbon dioxide (CO_2), 6.78% methane (CH_4), and 0.74% hydrogen (H_2). It is precisely because sawdust generates a large amount of reducing gas during pyrolysis that manganese dioxide can be reduced to manganous oxide. The third stage (> 450°C) is the carbonization stage of sawdust,[44] and the TG and DTG curves gradually tend to flatten out.

Thermodynamic Characteristics Analysis

The gases generated by sawdust pyrolysis under oxygen-free conditions are mainly composed of carbon dioxide (CO_2), carbon monoxide (CO), methane (CH_4), and hydrogen (H_2). CO_2 is mainly generated by the initial cleavage of uronic acid in hemicellulose and the decomposition of carboxyl in lignin; CO mainly comes from the pyrolysis of carbonyl and ether bonds in sawdust; CH_4 is the guaiacol-based type and the p-propyl type structural unit methoxyl group in lignin; during pyrolysis, H_2 is produced by the alkane cracking reaction and the aromatic condensation reaction.[11] Figure 4 shows the Gibbs free-energy diagram of the reactions of three reducing gas products (CO, CH_4, H_2) and biochar (C) with MnO_2 at different reaction temperatures during the pyrolysis of sawdust. From Fig. 4, it can be clearly seen that the Gibbs free-energy of reducing MnO_2 by four reducing substances is less than zero and decreases with the increase of temperature, which indicates that the increase of temperature is beneficial to the reduction of MnO_2. Combined with the thermogravimetric curve of sawdust, it can be seen that the reducing gases (CO, CH_4, H_2) and biochar (C) are produced by pyrolysis of sawdust at 300°C to 500°C. In this temperature range, these reducing substances undergo redox reactions with MnO_2 in low-grade pyrolusite. Therefore, from the point of view of chemical thermodynamics, it is also proved that the simultaneous reduction of pyrolusite by sawdust pyrolysis is feasible.

Orthogonal Experiments

Based on the design principle of the Box-Behnken central combined test, the effects of three factors on the leaching efficiency of manganese were analyzed that included proportion of sawdust mass (6–13%) (A), roasting temperature (350–600°C) (B) and roasting time (10–35 min) (C), and the results are shown in Table II.

Using the experimental data in Table II, the multiple regression fitting of manganese leaching efficiency was carried out by using Design Expert 12 software, and the model is shown in Eq. 2. According to the results of variance analysis, the regression equation is statistically significant (P value < 0.0001). The regression equation shows that proportion of sawdust mass, roasting temperature, and roasting time all have significant influence on manganese leaching efficiency, and the descending order of influence is proportion of sawdust mass, roasting temperature, and roasting time. Response surface analysis (RSM) is shown in Fig. 5.

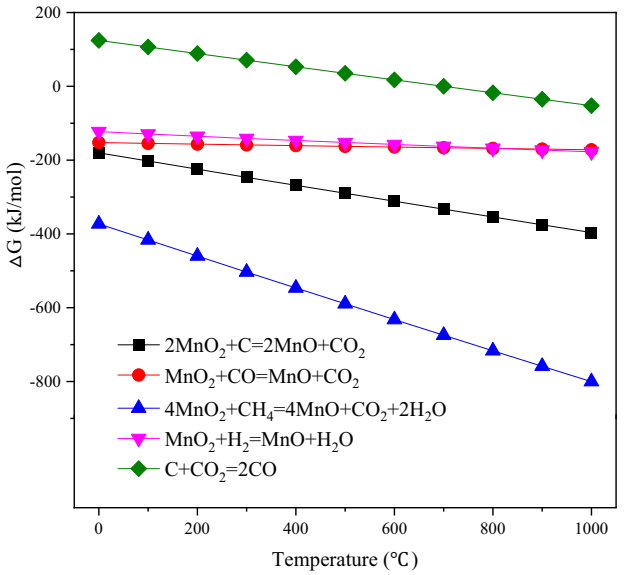

Fig. 4. Relationships between ΔG-T for main reactions of pyrolusite reduced by sawdust pyrolysis.

$$Y = 95.62 + 5.80A + 5.65B + 3.23C + 0.1250AB + 0.6225AC + 1.94BC - 4.82A^2 - 3.87B^2 - 3.67C^2 \quad (2)$$

Effect of Mass Ratio of Sawdust to Pyrolusite

In order to further optimize the influencing factors of manganese leaching efficiency, single factor experiments were conducted to investigate the effects of proportion of sawdust mass, roasting temperature, and roasting time on manganese leaching efficiency.

Under the conditions of roasting temperature of 500°C and roasting time of 30 min, the influence of sawdust dosage on manganese leaching efficiency was investigated. After roasting, the roasted products were leached with 1.5 mol/l sulfuric acid solution at 80°C for 120 min. The leaching efficiency of manganese was used to evaluate the influence of sawdust dosage. The experimental results are shown in Fig. 6.

From the experimental results in Fig. 6, it is obvious that the dosage of sawdust has a great influence on manganese leaching efficiency. With the increase of sawdust dosage, the leaching

Table II. Design and results of the orthogonal experiments

No.	A (%)	B (°C)	C (min)	Leaching efficiency of Mn (%)
1	6	350	22.5	75.32
2	13	350	22.5	86.37
3	6	600	22.5	87.03
4	13	600	22.5	98.58
5	6	475	10	77.08
6	13	475	10	87.73
7	6	475	35	85.09
8	13	475	35	98.23
9	9.5	350	10	82.87
10	9.5	600	10	89.65
11	9.5	350	35	82.64
12	9.5	600	35	97.17
13	9.5	475	22.5	95.65
14	9.5	475	22.5	95.48
15	9.5	475	22.5	95.77
16	9.5	475	22.5	95.59
17	9.5	475	22.5	95.62

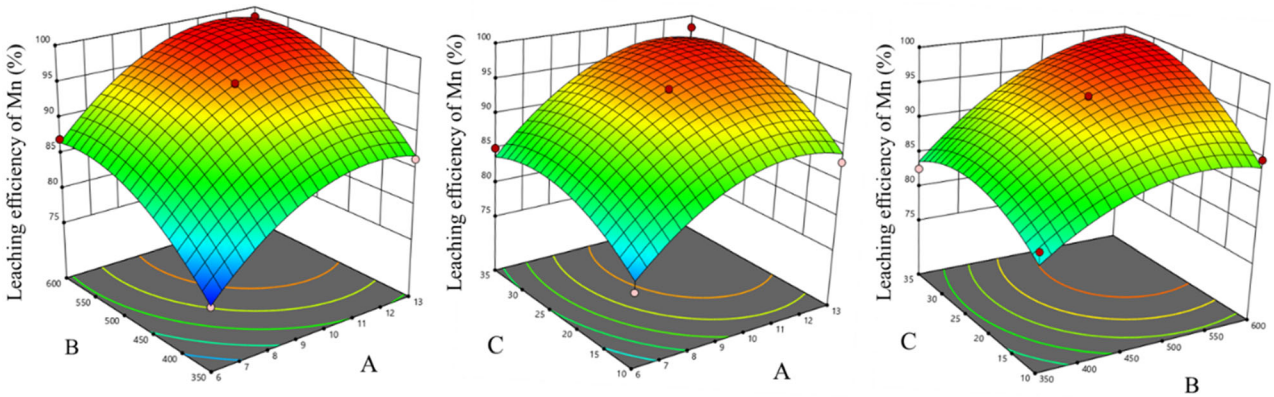

Fig. 5. Response surface of the influence of various factors on the manganese leaching efficiency. *A*, proportion of sawdust mass; *B*, roasting temperature; *C*, roasting time.

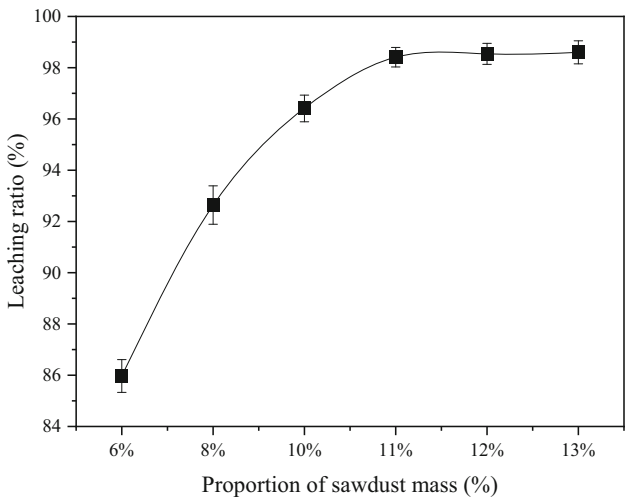

Fig. 6. Effect of sawdust dosage on manganese leaching ratio.

efficiency of manganese increased continuously. When the mass of sawdust was 6% of that of low-grade pyrolusite, the leaching efficiency of manganese was only 85.97%; when the dosage of sawdust increased to 11% of pyrolusite mass, the leaching efficiency of manganese increased by 12.45% to 98.42%. However, a phenomenon was found that the leaching efficiency of manganese remained basically unchanged when the sawdust dosage was further increased after 11%. Therefore, it was determined that the optimum dosage of sawdust was 11% of the low-grade pyrolusite.

In order to explore the phase transformation of low-grade pyrolusite with different sawdust dosages, the roasting products generated under different sawdust dosages were characterized by XRD, and the results are shown in Fig. 7. By comparing the XRD pattern of roasting product obtained with a sawdust mass ratio of 6% with the XRD pattern of low-grade pyrolusite (black line) in Fig. 7, it can be clearly seen that when the mass of

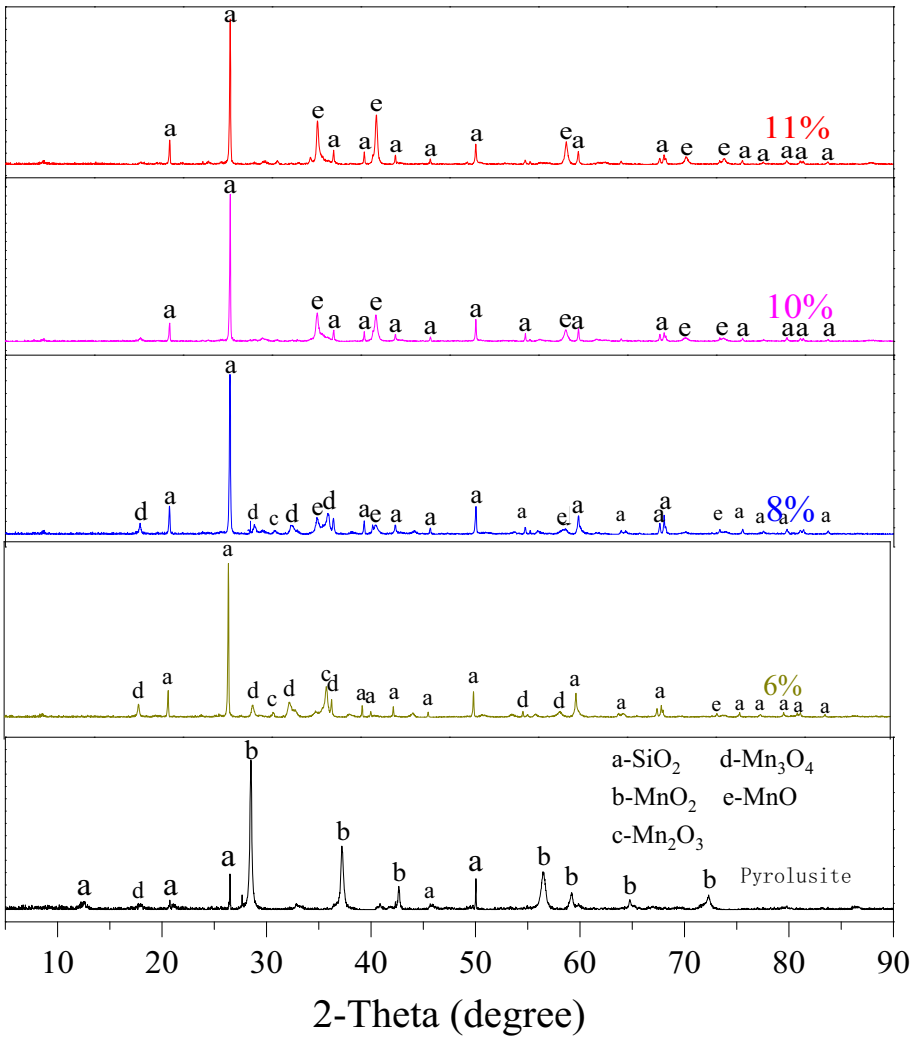

Fig. 7. XRD patterns of roasting products at different dosages of sawdust.

sawdust accounted for 6% of the mass of low-grade pyrolusite, the MnO_2 diffraction peak completely disappeared, while obvious diffraction peaks of Mn_2O_3 and Mn_3O_4, and a small amount of MnO diffraction peak were observed, which indicates that MnO_2 in low-grade pyrolusite was mainly reduced to Mn_2O_3 and Mn_3O_4 due to the lack of reducing gas. When the proportion of sawdust to low-grade pyrolusite was increased from 6% to 8%, the diffraction peaks of Mn_2O_3 and Mn_3O_4 in the roasting product were obviously reduced, while the diffraction peaks of MnO were further increased. It is precisely because of the increase of MnO phase in the roasting product that the leaching ratio of manganese was increased. Although the types of diffraction peaks of XRD patterns of roasting products with sawdust mass accounting for 10% and 11% of low-grade pyrolusite mass, respectively, were basically the same, when sawdust mass accounts for 11% of low-grade pyrolusite mass, the diffraction peaks of MnO were more obvious. The leaching ratio of manganese reached 98.42% with a sawdust dose of 11% of that of low-grade pyrolusite, because the MnO_2 in low-grade pyrolusite was basically completely reduced to MnO, which was effectively leached by dilute sulfuric acid.

Effect of Roasting Temperature

Based on the above results, the influence of roasting temperature on manganese leaching efficiency was studied under the conditions of sawdust dosage accounting for 11% of low-grade pyrolusite mass and roasting time of 30 min. After roasting, the roasted products were leached with 1.5 mol/l sulfuric acid solution at 80°C for 120 min. The experimental results are shown in Fig. 8.

It can be seen from Fig. 8 that with the increase of roasting temperature, the leaching efficiency of manganese was continuously improved. The roasting temperature was continuously raised from 350°C to 500°C, and the leaching efficiency of manganese continuously increased from 84.14% to 98.39%. After 500°C, the leaching efficiency of

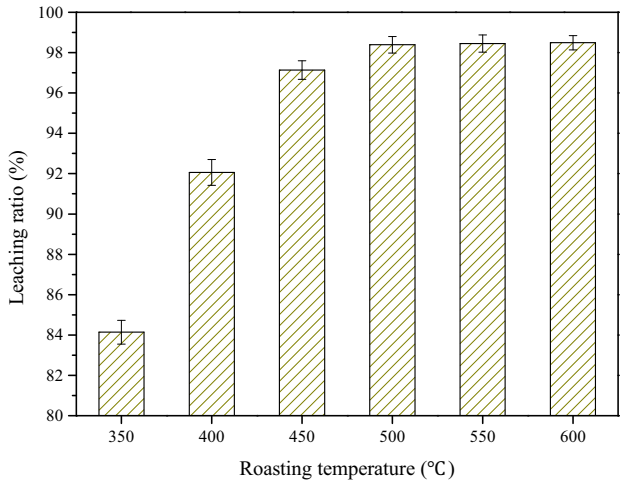

Fig. 8. Effect of roasting temperature on manganese leaching ratio.

manganese did not obviously increase with an increase of roasting temperature. However, an increase of temperature would increase the energy consumption, so the final optimal roasting temperature was chosen to be 500°C.

The XRD patterns of roasting products at different roasting temperatures are shown in Fig. 9. Comparing the XRD pattern of low-grade pyrolusite with the XRD pattern of the product roasted at 350°C for 30 min with a sawdust dose of 11% of the low-grade pyrolusite, the XRD pattern of the roasting product obtained at 350°C showed mainly the diffraction peaks of Mn_2O_3, Mn_3O_4, and SiO_2, which shows that the reducing substances produced by sawdust pyrolysis at this temperature could reduce MnO_2 in low-grade pyrolusite to Mn_2O_3 and Mn_3O_4. When the roasting temperature was raised to 400°C, the diffraction peak of Mn_2O_3 basically disappeared, while a small amount of MnO diffraction peak was observed. According to the results of thermogravimetric analysis of sawdust (Fig. 3), the temperature range of rapid pyrolysis of sawdust is between 350°C and 400°C, so more reducing substances are generated. At the same amount of sawdust and roasting time, the number and intensity of diffraction peaks of MnO in roasting product increased when the roasting temperature was raised to 450°C, compared with that when the roasting temperature was 400°C. However, at this roasting temperature, the diffraction peak of Mn_3O_4 can still be obviously observed. From the XRD pattern of the roasting product at 500°C in Fig. 9, it can be seen that only diffraction peaks of MnO and SiO_2 can be observed in the roasting product, which shows that the process of simultaneous reduction of low-grade pyrolusite by sawdust pyrolysis has been basically completed. Although the diffraction peak of MnO was more obvious at 550°C, the leaching efficiency of manganese was basically the same as that at 500°C.

Effect of Roasting Time

In order to study the best technological conditions for simultaneous reduction of low-grade pyrolusite by sawdust pyrolysis, the effects of roasting times of 10 min, 15 min, 20 min, 25 min, 30 min, and 35 min on manganese leaching efficiency were investigated under the conditions of sawdust dosage of 11% of low-grade pyrolusite mass and roasting temperature of 500°C. The leaching conditions of roasted products were sulfuric acid concentration of 1.5 mol/l, leaching temperature of 80°C and leaching time of 120 min. The experimental results are shown in Fig. 10.

It can be seen from Fig. 10 that the rate of simultaneous reduction of low-grade pyrolusite by sawdust pyrolysis was fast, and the leaching efficiency of manganese was 87.68% when the roasting time was only 10 min. With the prolongation of roasting time, the leaching efficiency of manganese increased rapidly. When the roasting time was increased to 25 min, the leaching efficiency of manganese reached 98.45%. However, if the roasting time was further prolonged after 25 min, the leaching efficiency of manganese remained relatively stable, but the energy consumption was increased. Therefore, according to the experimental results, the final optimum roasting time of 25 min was selected.

Based on the analysis of the above single-factor experiments, the final reduction roasting conditions were as follows: the sawdust dosage is 11% of the mass of low-grade pyrolusite, the roasting temperature is 500°C, and the roasting time is 25 min. Under these conditions, the leaching efficiency of manganese is kept above 98% with 1.5 mol/l sulfuric acid solution as the leaching agent.

Analysis of Reaction Mechanism

Based on the analysis of the pyrolysis characteristics of sawdust, the thermodynamic characteristics of reduction roasting, the quality index, and the phase change of roasted products, the mechanism for recovering manganese from low-grade pyrolusite by the sawdust pyrolysis reduction roasting-acid leaching process was put forward. The mechanism diagram is shown in Fig. 11.

Under medium and low temperature conditions, sawdust is pyrolyzed into biomass carbon (C), carbon dioxide (CO_2), carbon monoxide (CO), methane (CH_4), hydrogen (H_2), water vapor (H_2O), etc., among which biomass carbon (C), carbon monoxide (CO), methane (CH_4), and hydrogen (H_2) are used as reducing substances. The whole pyrolysis process of sawdust can be regarded as the linear superposition of the pyrolysis processes of cellulose, hemicellulose, and lignin. The pyrolysis products of cellulose and hemicellulose are mainly volatile substances, and lignin is mainly decomposed into biomass carbon. As shown in Fig. 11, the mechanism of synchronous reduction of low-grade

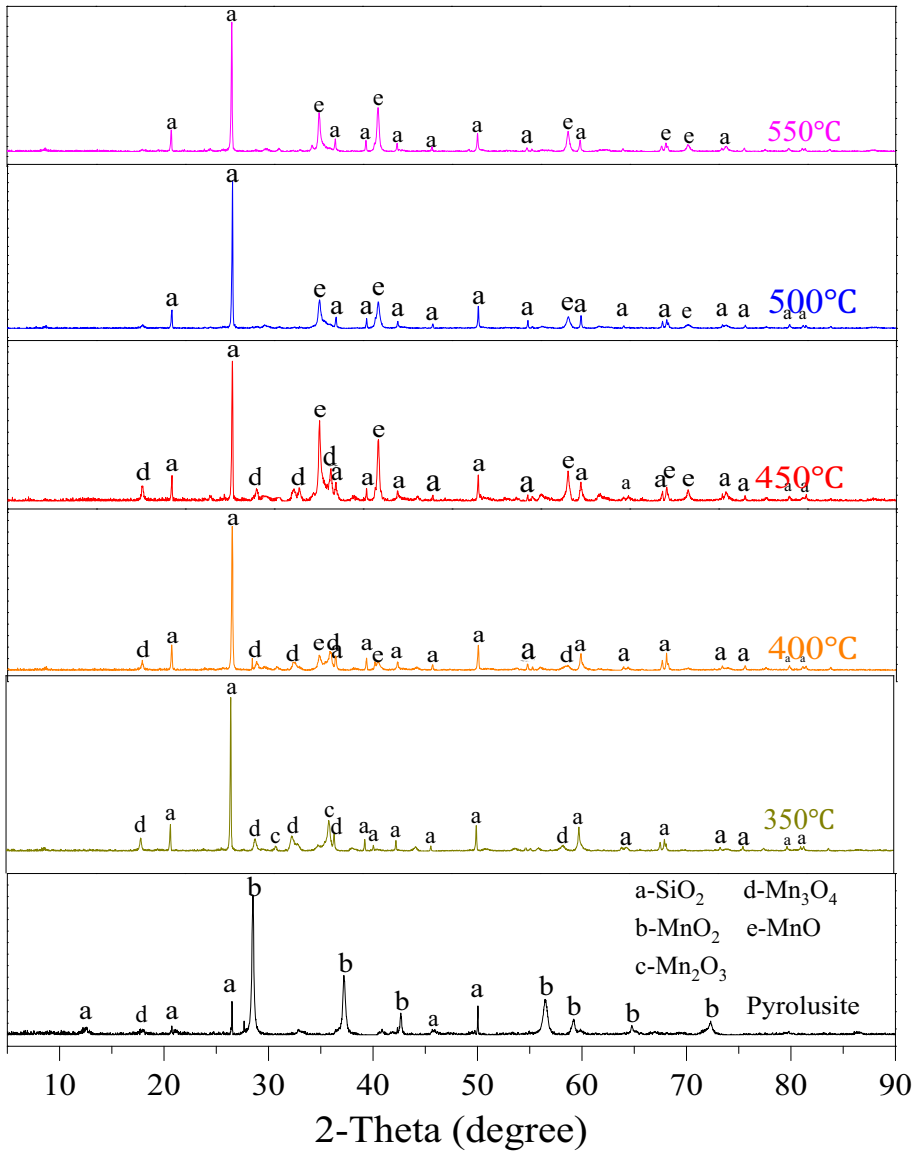

Fig. 9. XRD patterns of roasting products at different roasting temperatures.

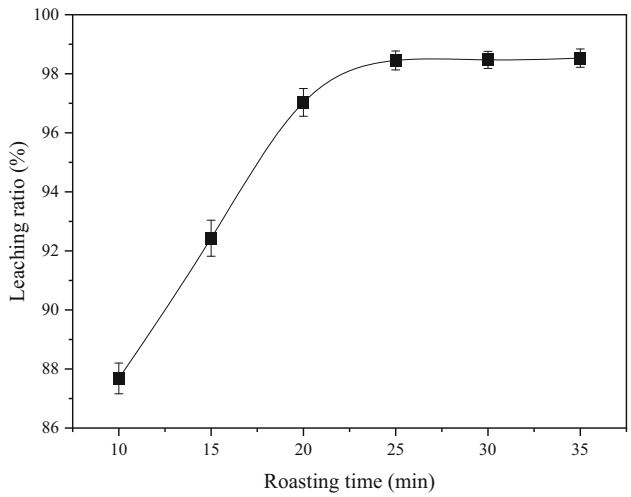

Fig. 10. Effect of roasting time on manganese leaching ratio.

pyrolusite by sawdust pyrolysis can be divided into two components: biomass pyrolysis and low-grade pyrolusite reduction; that is, biomass pyrolysis first produces reducing components, and then the manganese dioxide (MnO_2) in low-grade pyrolusite reacts with reducing components, which mainly include fixed carbon (C), carbon monoxide (CO), methane (CH_4), and hydrogen (H_2). The reduction process of manganese dioxide (MnO_2) in low-grade pyrolusite is divided into three steps. First, the reducing substance generated by the pyrolysis of sawdust reduces MnO_2 to Mn_2O_3, then Mn_2O_3 is gradually reduced to Mn_3O_4, and finally the reducing substance reduces Mn_3O_4 to MnO. When MnO_2 in low-grade pyrolusite is completely reduced to MnO, manganese can be extracted by sulfuric acid leaching. Compared with traditional anthracite reduction, biomass reduction has the characteristics

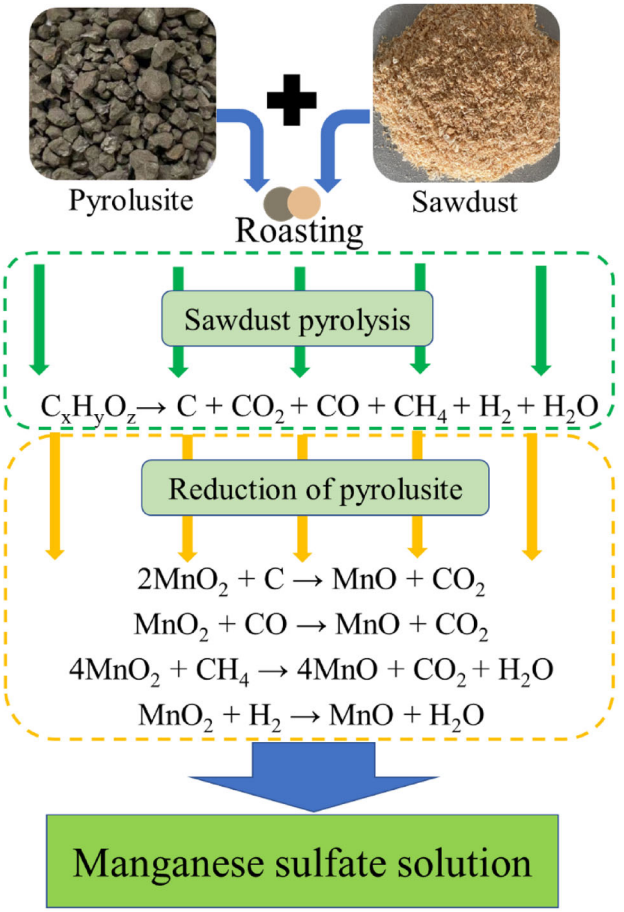

Fig. 11. The mechanism diagram for extraction of manganese from low-grade pyrolusite by the sawdust pyrolysis reduction roasting-acid leaching process.

of fast reduction rate, low reduction temperature, and low energy consumption, which is conducive to improving energy efficiency and working conditions.

CONCLUSION

In this work, a method for extraction of manganese from low-grade pyrolusite by a sawdust pyrolysis reduction roasting-acid leaching process was explored. Compared with traditional coal as the reducing agent, the biomass reduction process has lower energy consumption and higher efficiency. The reduction process of low-grade pyrolusite by sawdust can not only maximize the utilization of biomass energy and save the consumption of traditional coal resources, but also achieve efficient extraction of manganese. Sawdust is rapidly pyrolyzed at 250–450°C to generate a large amount of reducing gases such as carbon monoxide (CO), methane (CH_4), hydrogen (H_2) and biochar (C), and these reducing substances gradually reduce manganese dioxide (MnO_2) in low-grade pyrolusite to manganous oxide (MnO). The reduction process of MnO_2 is identified as $MnO_2 \rightarrow Mn_2O_3 \rightarrow Mn_3O_4 \rightarrow MnO$. Under the conditions that the sawdust dosage was 11% of the mass of low-grade pyrolusite, the roasting temperature was 500°C, and the roasting time was 25 min, the leaching efficiency of manganese reached 98.45% with 1.5 mol/l sulfuric acid solution as the leaching agent.

ACKNOWLEDGEMENTS

This research was supported by China Ocean Mineral Resources R&D Association under Grant No. JS-KTHT-2019-01. In addition, I would like to thank my girlfriend Lina Ma (Xi'an Shiyou University) for her encouragement during the writing of this paper.

CONFLICT OF INTEREST

There are no conflict to declare.

REFERENCES

1. J. Zhao, K. Dong, X. Dong, and M. Shahbaz, *Renew Energy* 186, 299 (2022).
2. R. Yasmeen, C. Zhuhai, W.U. Hassan Shah, M.A. Kamal, and A. Khan, *Energy*. https://doi.org/10.1016/j.energy.2021.122703 (2021).
3. N. Hajinajaf, A. Mehrabadi, and O. Tavakoli, *Biomass Bioenergy.* 145, 105941 (2021).
4. S.L. Narnaware and N.L. Panwar, *Bioresour. Technol. Rep.* 17, 100892 (2022).
5. R. Wei, S. Feng, H. Long, J. Li, Z. Yuan, D. Cang, and C. Xu, *Energy* 140, 406 (2017).
6. K.B. Ansari, B. Kamal, S. Beg, M.A. Wakeel Khan, M.S. Khan, M.K. AlMesfer, and M. Danish, *Renew. Sust. Energy Rev.* 150, 111454 (2021).
7. A. Demirbaş, *Energy Convers. Manage.* 41, 633 (2000).
8. H. Suopajärvi, E. Pongrácz, and T. Fabritius, *Renew. Sust. Energy Rev.* 25, 511 (2013).
9. R. Yue, X. Zhang, Y. Zhong, Z. Chen, Y. Zhao, D. Wang, Z. Wang, and X. Mao, *J. Hazard Mater.* 423, 126937 (2022).
10. D.B. Huang, Y.B. Zong, R.F. Wei, W. Gao, and X.M. Liu, *J. Iron Steel Res. Int.* 23, 874 (2016).
11. J. Du, L. Gao, Y. Yang, S. Guo, M. Omran, J. Chen, and G. Chen, *Fuel* 305, 121546 (2021).
12. K. Li, Q. Jiang, G. Chen, L. Gao, J. Peng, Q. Chen, S. Koppala, M. Omran, and J. Chen, *Bioresour. Technol.* 319, 124172 (2021).
13. J. Han and H. Kim, *Renew. Sust. Energy Rev.* 12, 397 (2008).
14. D. Duan, D. Chen, L. Huang, Y. Zhang, Y. Zhang, Q. Wang, G. Xiao, W. Zhang, H. Lei, and R. Ruan, *J. Anal. Appl. Pyrol.* 158, 105246 (2021).
15. X.B. Zheng, P. Li, S.X. Dou, W.P. Sun, H.G. Pan, D.S. Wang, and Y.D. Li, *Energy Environ. Sci.* 14, 2809 (2021).
16. S. Luo, H. Guo, S. Zhang, Z. Wang, X. Li, W. Peng, J. Wang, and G. Yan, *J. Clean Prod.* 326, 129266 (2021).
17. H. Zheng, G. Wu, G. Gao, and X. Wang, *Chem. Eng. J.* 421, 129606 (2021).
18. S. He, D. Jiang, M. Hong, and Z. Liu, *J. Clean Prod.* 306, 127224 (2021).
19. S. Lin, L. Gao, Y. Yang, J. Chen, S. Guo, M. Omran, and G. Chen, *Hydrometallurgy* 198, 105519 (2020).
20. J. Ju, Y. Feng, H. Li, X. Li, Q. Zhang, C. Xu, and S. Liu, *Environ. Technol. Inno.* 24, 101903 (2021).
21. K. Li, J. Chen, G. Chen, J. Peng, R. Ruan, and C. Srinivasakannan, *Bioresour. Technol.* 286, 121381 (2019).
22. X.Y. Deng, Y.L. Feng, H.R. Li, Z.W. Du, J.X. Kang, and C.L. Guo, *T. Nonferr. Metal Soc.* 28, 1045 (2018).
23. D. Vamvuka, E. Kakaras, E. Kastanaki, and P. Grammelis, *Fuel* 82, 2003 (1949).
24. Y. Du, W. Qi, X. Miao, G. Li, and C. Hu, *J. Chem. Ind. Eng. (China).* 55, 2099 (2004).
25. Y.L. Feng, S.Y. Zhang, and H.R. Li, *Int. J. Min. Met. Mater.* 23, 241 (2016).

26. A.A. Ismail, E.A. Ali, A. Ibrahim, and M.S. Ahmed, *Can. J. Chem. Eng.* 82, 1296 (2004).
27. Q. Ye, J. Chen, G. Chen, J. Peng, C. Srinivasakannan, and R. Ruan, *Adv. Powder Technol.* 29, 2018 (1871).
28. S. Lin, K. Li, Y. Yang, L. Gao, M. Omran, S. Guo, J. Chen, and G. Chen, *Chem. Eng. Process.* 159, 108209 (2021).
29. S. Lin, L. Gao, Y. Yang, J. Chen, S. Guo, M. Omran, and G. Chen, *J. Mater. Res. Technol.* 9, 13128 (2020).
30. Z. You, G. Li, J. Dang, W. Yu, and X. Lv, *Powder Technol.* 330, 310 (2018).
31. P. Perreault and G.S. Patience, *Chem. Eng J.* 295, 227 (2016).
32. H. Wu, Y. Feng, H. Li, H. Wang, and J. Ju, *Chem. Eng. Process.* 147, 107742 (2020).
33. X.Y. Zhang, X.D. Tian, and D.F. Zhang, *T. Nonferr. Metal Soc.* 16, 705 (2006).
34. H. Su, Y. Wen, F. Wang, Y. Sun, and Z. Tong, *Hydrometallurgy* 93, 136 (2008).
35. M.K. Sinha and W. Purcell, *Hydrometallurgy* 187, 168 (2019).
36. K.D. Yang, X.J. Ye, J. Su, H.F. Su, Y.F. Long, X.Y. Lü, and Y.X. Wen, *T. Nonferr. Metal Soc.* 23, 548 (2013).
37. Q. Tang, H. Zhong, S. Wang, J.Z. Li, and G.Y. Liu, *T. Nonferr. Metal Soc.* 24, 861 (2014).
38. C.X.Y. Zhou, T. Li, T.X. Xie, and Y.K. Zhang, *Desalin. Water Treat.* 57, 16822 (2016).
39. K. Li, G. Chen, X. Li, J. Peng, R. Ruan, M. Omran, and J. Chen, *Bioresour. Technol.* 294, 122217 (2019).
40. J. Du, L. Gao, Y. Yang, G. Chen, S. Guo, M. Omran, J. Chen, and R. Ruan, *Bioresour. Technol.* 324, 124660 (2021).
41. Y. Long, L. Ruan, X. Lv, Y. Lv, J. Su, and Y. Wen, *Chin. J. Chem. Eng.* 23, 1691 (2015).
42. C. Di Blasi, *Prog. Energy Combust.* 34, 47 (2008).
43. K. Li, G. Chen, J. Chen, J. Peng, R. Ruan, and C. Srinivasakannan, *Bioresour. Technol.* 291, 121838 (2019).
44. M.N. Lapuerta, J.J. Hernández, and J.N. Rodriguez, *Biomass Bioenergy* 27, 385 (2004).